Number Size Distribution of Atmospheric Particles in a suburban Beijing in the Summer and Winter of 2015

Du, Peng; Gui, Huaqiao; Zhang, Jiaoshi; Liu, Jianguo; Yu, Tongzhu; Wang, Jie; Cheng, Yin; Shi, Zongbo

DOI:
10.1016/j.atmosenv.2018.05.023

Number Size Distribution of Atmospheric Particles in a suburban Beijing in the Summer and Winter of 2015

Peng Du[1,2], Huaqiao Gui[1,3], Jiaoshi Zhang[1*], Jianguo Liu[1,3*], Tongzhu Yu[1], Jie Wang[1], Yin Cheng[1], Zongbo Shi[4]

1. Key Laboratory of Environmental Optics and Technology, Anhui Institute of Optics and Fine Mechanics, Chinese Academy of Sciences, Hefei 230031, China

2. University of Chinese Academy of Sciences, Beijing 100049, China

3. Center for Excellence in Regional Atmospheric Environment, Institute of Urban Environment, Chinese Academy of Sciences, Xiamen 361021, China

4. School of Geography, Earth and Environmental Sciences, University of Birmingham, Edgbaston, Birmingham, B15 2TT, United Kingdom

Abstract. Particle number size distribution in a suburban Beijing was measured during the HOPE-J3A (Haze Observation Project Especially for Jing–Jin–Ji Area) field campaigns in 2015 from 18 June to 23 July (summer) and 2 to 25 December (winter). Average particle concentrations during the summer and winter campaigns were $9.6\pm4.8\times10^3 cm^{-3}$ and $13.9\pm8.3\times10^3 cm^{-3}$, respectively. Particle numbers were dominated by Aitken mode particles in both seasons. During the winter campaign, pollution events occurred every four to five days, each lasting for two to three days. In contrast, pollution events lasted for one to two days every six to seven days during the summer campaign. Aitken mode particles were 50% higher in the winter but new particle formation (NPF) events occurred more frequently in the summer. NPF events usually starts at around 10:00 LT (local time) in the summer but 12:00 LT in the winter. Aitken and accumulation mode particles accounted for 43.5% and 38.2% of all particles. The proportion of Aitken mode to total particles remained almost the same during summer, while it increased as haze intensified in winter. Particle number concentration was closely correlated with traffic and residents living activities and

wind speed, with higher concentrations during rush hours, heating period and in the southerly wind. These results, when combined with trajectory cluster analysis, suggest that Aitken and accumulation mode particles were mainly from regional transport during the summer campaign, but from vehicle and coal-combustion emissions during the winter campaign.

Key words: Particle Number Size distribution, Beijing, aerosol, Trajectory Cluster Analysis, New Particle Formation

1. Introduction

Aerosol particles play an important role in the atmosphere because of their significant effects on air quality, visibility (Watson, 2002), direct and indirect climate forcing (Anderson et al., 2003; Andreae and Rosenfeld, 2008; Bahadur et al., 2012; Mahowald, 2011; Ramanathan et al., 2001), the environment (Cao et al., 2013; Huang et al., 2014) and human health (Nel, 2005; Tang et al., 2017; Zheng et al., 2014). Accordingly, these particles have received a great deal of attention from the government and the general public. The rapid economic and industrial development and urbanization that have occurred in China have brought about serious environmental problems in Chinese megacities, especially in the Beijing–Tianjin–Hebei region, the Yangtze River delta, and the Pearl River delta (Chan and Yao, 2008; Gao et al., 2009; Han et al., 2015; Parrish and Zhu, 2009; Zhuang et al., 2014). As the capital of China and a rapidly developing city, Beijing has been experiencing severe haze pollution for years. Despite many measures taken by the government to address this issue (Sun et al., 2016; Tang et al., 2015; Wang et al., 2010; Xu et al., 2016a), air pollution is not improving as rapidly as it could. The $PM_{2.5}$ in Beijing is still abnormally elevated, and often greatly exceeds the level of 75 μgm^{-3} considered by the China National Ambient Air Quality Standard (NAAQS) to be harmful to health (Ji et al., 2014; Xu et al., 2016b; Zhang et al., 2013).

Measurements of particle number size distributions have been conducted

worldwide (Gao et al., 2012; Gao et al., 2009; Hussein et al., 2004; Quan et al., 2014; Stanier et al., 2004; Wehner and Wiedensohler, 2003; Zhang et al., 2016). When compared with rural areas and background areas, the concentrations of atmospheric particles in urban areas is higher (Wehner and Wiedensohler, 2003; Hussein et al., 2004). Moreover, the concentration of atmospheric particles in winter in urban areas was higher than that in summer, and the diurnal variation of atmospheric particles was significantly influenced by traffic emissions. To study the formation and evolution of atmospheric particles in Beijing, many scholars have conducted observations and experiments investigating the number concentration distribution of atmospheric aerosols. However, most of these have only focused on a pollution process or unique period (An et al., 2007; Liu et al., 2017; Sun et al., 2014; Tang et al., 2015; Wang et al., 2010; Wang et al., 2014c; Xin et al., 2010; Zhang et al., 2017). The seasonal variation of particle number size distribution can reflect the periodic pollution process to a certain extent, such as the higher frequency of haze in winter than that in summer. The distribution of particles under different pollution conditions may demonstrate implicit links to the pollution source (Wang et al., 2014b). The new particle formation (NPF) is one of the important sources of atmospheric particles and cloud condensation nuclei. The NPF events also exhibits a regular seasonal variation (Wu et al., 2007). Studying the characteristics and mechanisms of NPF will help to further understand the climatic, environmental and health effects of atmospheric particulates. In addition, meteorological parameters such as wind direction temperature and wind speed play an important role in influencing the particle number size distribution, accounting for about 37% of all factors. Because of the typical warm temperate semi-humid continental monsoon climate, hot and rainy summer, and cold and dry winter, it had a significant impact on the distribution of particles in Beijing (Liang et al., 2017; Schäfer et al., 2013; Sun et al., 2015). Moreover, regional transport plays an important role in changing the particle number concentrations (Chen et al., 2017; Zhu et al., 2016). The meteorological parameters could alter the size disturbution of atmspheric particles, which may signify the potential sources of the particles--local emissions and regional transport.

Here, we report continuous measurements of the particle size distribution of aerosols at a suburban site (Huairou) during winter and summer in 2015. The influence of meteorological parameters, especially wind speed and direction, on the particle number size distributions of atmospheric aerosols was analyzed. The mixed single-particle Lagrangian integral transport and diffusion model (HYSPLIT) developed by the Ocean Resources and Atmospheric Administration (NOAA) Air Resources Laboratory (ARL) was used to simulate the trajectories of air masses reaching the observation points during summer and winter. The correlation between different mode particles and local emissions as well as regional transport were then investigated.

2. Methodology

The observations took place at the Yanqi Lake campus of the University of Chinese Academy of Sciences (UCAS), which is located in the Huairou District, northeastern Beijing (40°24′24.45″N, 116°40′32.95″E), as shown in Figure 1. The summer campaign was from 18 June to 23 July and winter from 2 to 25 December 2015. Due to the SMPS was broke down from 15 to 21 December 2015, the data for this period was missing. The Yanqi Lake Campus of the UCAS is about 50 km away from the central Beijing. The campus is located at the junction of Yanshan Mountain and the North China Plain (NCP), where northwest airflow and south air flow converge, making it easy to observe the impact of regional transport. The observation site is adjacent to China National Highway 111 and a rural residential area. The instruments were installed on the top floor of Teaching Building 1, with the sample inlet about 1.5 m above the roof.

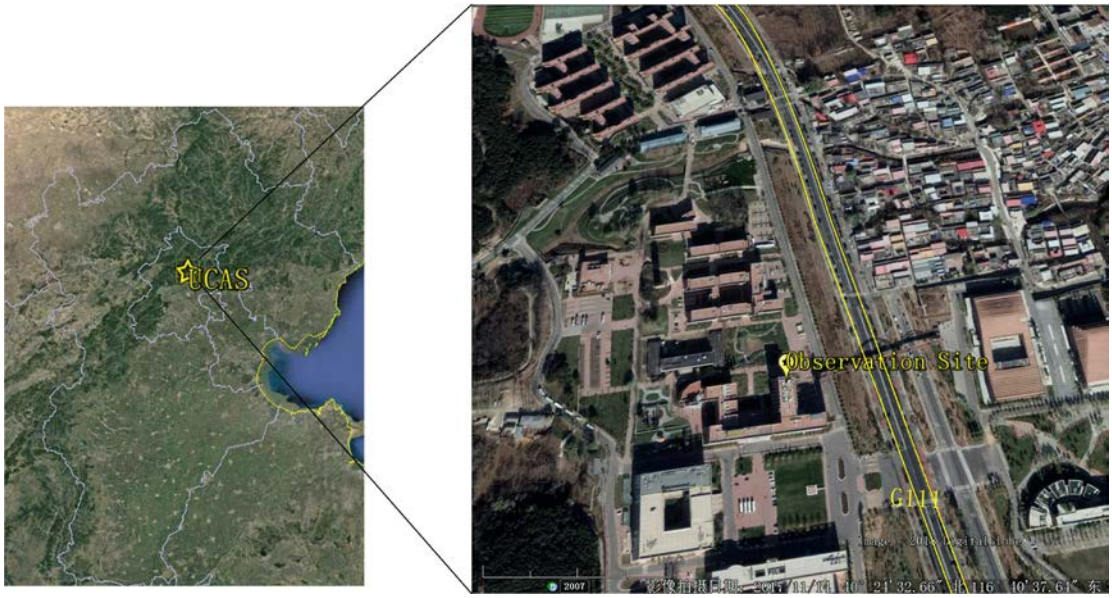

Figure 1. The map of the North China Plain. The observation site (UCAS) is marked with yellow balloon sign.

The particle number size distributions of the aerosols between 11.1 and 1083.3 nm was measured every 7 mins using a scanning mobility particle sizer (SMPS, Grimm Aerosol Technik Gmbh, Germany, Model 5.400), which consists of an Am-241 neutralizer (Model 5.522), a long Vienna-type differential mobility analyzer (L-DMA, model 55-990) and a condensation particle counter (CPC, model 5.403)(Heim et al., 2004). The size distribution inversion was conducted using the manufacturer-provided software (GRIMM 5.477 Version 1.35) developed and described in detail by Reischl (1991). Diffusion losses and the effects of multi-charged particles were corrected using the instrument software. The SMPS was validated with laboratory-generated, commercially available certified (Duke Standard) NIST-traceable monodispersed polystyrene latex (PSL) particles of two known sizes, 203±5nm and 499±8nm, before and after the campaign (Joshi et al., 2012). The deviation between measured particle sizes and the certified diameters of the PSL spheres agreed to within 4%. Considering the uncertainty in PSL size and other possible experimental uncertainties, the results were well within the confidence required to proceed further. Atmospheric aerosols were divided into nucleation mode (<25 nm), Aitken mode (25-100 nm), accumulation mode (0.1-1 μm) to calculate the concentrations in different size categories.

The ambient aerosols were dried to a RH below 20% using a Nafion drier (MD-700; Perma Pure LLC), then passed into the SMPS as the sample flow. The RH of the sheath flow of SMPS was dried to below 20% using a diffusion drier, then passed through a HEPA filter before being sent to the DMA. The temperature and humidity of the sample flow and sheath flow were measured using a digital humidity and temperature sensor (SHT11; Sensirion China Co., Ltd) and logged every minute to ensure that the aerosol size distributions were measured under dry conditions; therefore, hygroscopic growth was not considered.

The Hybrid Single-Particle Lagrangian Integrated Trajectory (HYSPLIT) model developed by NOAA/ARL (National Oceanic and Atmospheric Administration/Air Resources Laboratory) was used to calculate the backward trajectories of air masses arriving at the observation site during summer and winter campaigns. The mode data comes from the GDAS observations of the National Environmental Prediction Center of the United States. The 36-h backward trajectories starting at 200 m were calculated every 6 hours (at 00:00, 06:00, 12:00, 18:00). Then the built-in cluster analysis tool of HYSPLIT was used to group the air mass trajectories according to the spatial total variance (TSV).

The meteorological parameters, including wind speed and direction, temperature, relative humidity, and atmospheric pressure, were continuously recorded by a MetPak automatic weather station (Gill Instruments Ltd., Lymington, UK). Moreover, the wind profiles from 40 to 320m were also recorded by a Doppler wind lidar (Windcube 8, Leosphere, Orsay, France). The hourly average values of mass concentrations of $PM_{2.5}$ and pollutant gases (SO_2, NO_2, O_3, and CO) were retrieved from the China National Environmental Monitoring Center National Urban Air Quality Real-time Release Platform (http://113.108.142.147:20035/emcpublish).

3. Results and discussion

3.1 Overview of particle number size distribution

An overview of the measurement results of the aerosol size distribution, mass

concentration of $PM_{2.5}$ and gaseous pollutants is shown in Figure 2. Particle number concentrations showed periodic behavior, with lower concentrations being observed in summer and higher in winter. Particle number concentrations are well correlated to $PM_{2.5}$ mass concentrations. Mass concentration of $PM_{2.5}$ during the winter campaign was 122.9±123.4 μg m^{-3}, which was almost two times higher than that during the summer campaign (66.4±50.2 μg m^{-3}). Periodic pollution process was observed every four to five days, each lasting for two to three days during the winter campaign, whereas they only lasted for one to two days every six to seven days during the summer campaign. The frequency of new particle formation (NPF) events was higher during summer and subsequently accompanied by a significant growth process. Mass concentration of $PM_{2.5}$ increased with the NPF and subsequent growth process. The correlation coefficient between NO_2 and $PM_{2.5}$ was 0.75 as well as CO and $PM_{2.5}$ were well correlated with 0.86, indicating a significant contribution from the primary emissions.

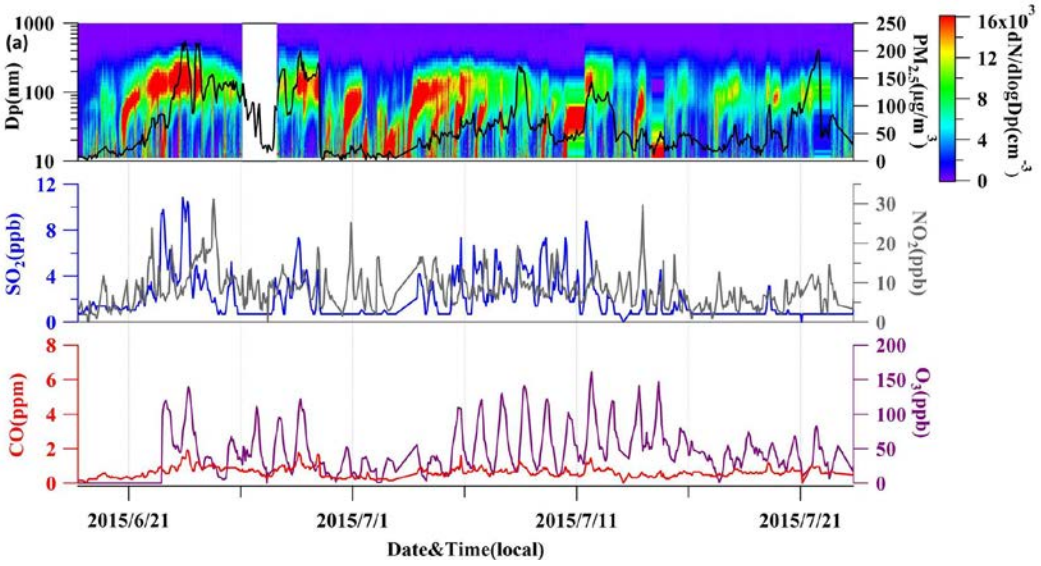

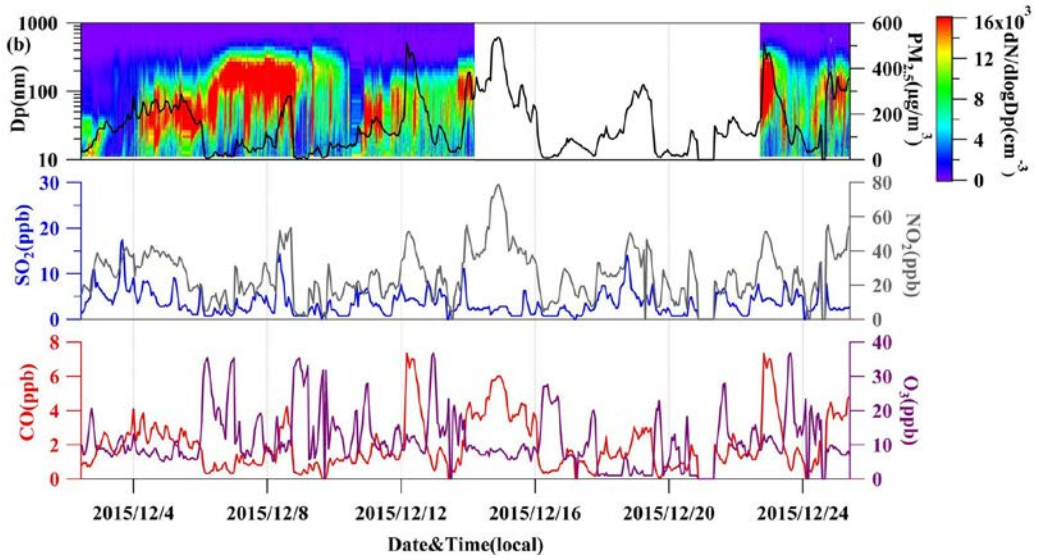

Figure 2. Time series of aerosol number size distribution measured by SMPS, mass concentrations of $PM_{2.5}$ and gaseous pollutants (SO_2, NO_2, O_3, and CO) during the summer (a) and the winter (b) campaigns.

Figure 3 shows the statistical variations of particle number concentrations of nucleation, Aitken and accumulate mode and total number concentration during the summer and winter. Mean total number concentration of particles in the winter was $13.9\pm8.3\times10^3$ cm^{-3}, which was 45% higher than that during summer ($9.6\pm4.8\times10^3$ cm^{-3}). Aitken mode particles contributed 46% and 48% to total particle numbers in the summer and winter, following by accumulation (35% and 34%) and nucleation mode (19% and 18%) particles. Number concentration of Aitken mode particles were 50% higher in the winter than that in the summer, whereas nucleation and accumulation mode particles were 43.5% and 38.2% higher.

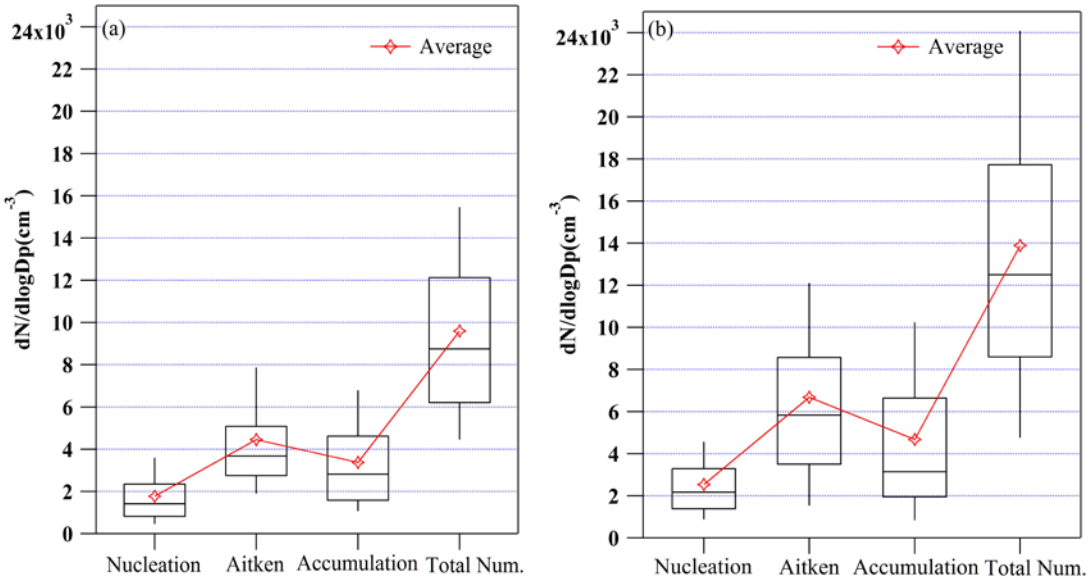

Figure 3. Box plots showing the statistical variations of particle number concentrations during the summer (a) and the winter (b).

Figure 4 shows the statistical variations in the size, surface area and volume distributions of particles below 1 μm at the Huairou site during the summer and winter of 2015. More than 99.5% of the particles are below 500 nm; Accumulation mode particles in the range of 100–500 nm made a significant contribution to the total surface area and volume. Furthermore, a significant >1 μm coarse mode in the volume was also observed. We also observed a peak between 100 and 200 nm in the winter and the summer, which has comparable average number concentrations. A significant peak between 40 and 50 nm was also seen during the winter, with an even higher number concentration that thot between 100–200 nm. Since the number concentration of the Aitken mode particles is affected by the primary emissions from transportation sources(Liu et al., 2017), it can be concluded that the observation site is more affected by local primary emission in the winter. The residence time of large particles is usually short, and they are easily removed by dry and wet sedimentation, so the concentration of particles beyond 500 nm is similar during winter and summer. The peak values of surface area concentration and volume concentration during the summer and the winter were similar, between 200–300 nm and 300 nm, respectively, but the concentrations in the winter were much higher than that in the summer.

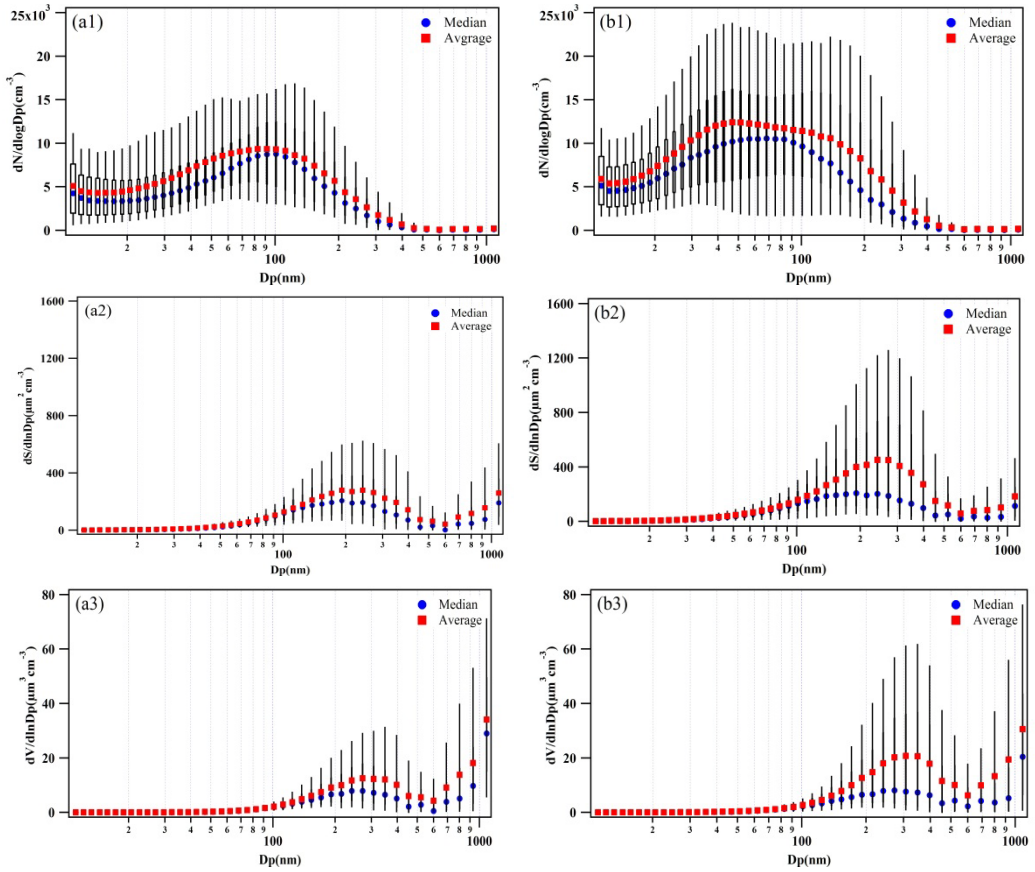

Figure 4. Box plots showing the particle number size distribution observed during the summer and the winter (a1, b1); and the size distribution of surface area (a2, b2) and volume (a3, b3) calculated from the number size distribution.

3.2 Diurnal variations of particle number size distributions

Figures 5 and 7 show the average diurnal variation of number size distributions of total, and nucleation, Aitken and accumulation mode particles during the two campaigns. Many factors influence the diurnal variation of the particle number size distributions, including the formation of secondary particles, local primary emissions, and meteorological conditions (Liu et al., 2016; Shen et al., 2011; Wu et al., 2008). The SO_2 concentration tended to increase as the nucleation mode particles, which indicated that the formation of secondary particles was the main contributor to the concentration of nucleation mode particles (Gao et al., 2012; Sun et al., 2016; Wang et al., 2013; Yue et al., 2009). The newly formed particles can grow through condensation and collision to Aitken mode even accumulation mode particles (Zhang et al., 2017). Motor vehicle exhaust, coal-combustion and other primary sources also

contribute to particle number concentrations (Liu et al., 2017; Wu et al., 2008).

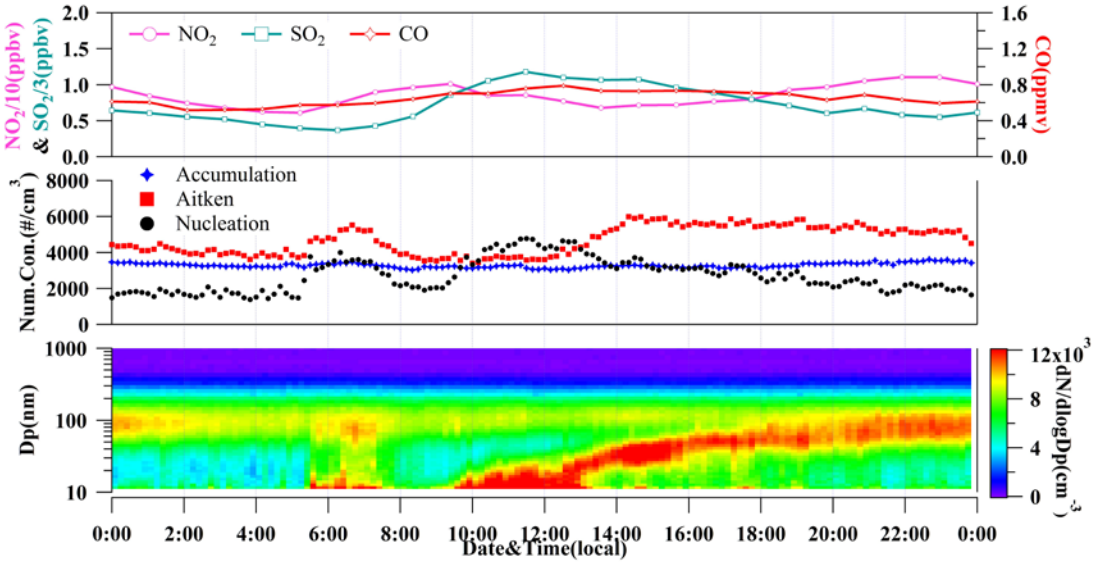

Figure 5. Average diurnal variation of NO_2, SO_2, CO concentrations and number size distributions of particles observed during the summer campaign.

Figure 5 shows that there is a significant increase in the average number concentration of particles, mainly in the nucleation and Aitken mode, in the morning from 6:00 to 8:00 h during the summer campaign; meanwhile, the NO_2 concentration increased, which was probably caused by motor vehicle exhaust emissions during morning rush hour (Wang et al., 2014c; Wu et al., 2008). After the morning peak, the concentration of nucleation and Aitken mode particles decreased to a level similar to those before the morning peak. From about 10:00 h onwards, the concentration of nucleation mode particles began to increase sharply, while that of the Aitken mode particles remained at a similar level. When the newly formed particles grew, the concentration of nucleation mode particles began to decrease, whereas that of the Aitken mode particles increased rapidly. Because the atmospheric nucleation process usually lasts for several hours, the increase in the concentration of particles in Aitken mode usually lagged behind that of nucleation mode particles (Kulmala, 2003; Kulmala et al., 2013; Kulmala et al., 2007). Following NPF, the particle size growth continued until the night, reaching about 80 nm, after which the concentration decreased. The NPF showed a “banana shape” in the diurnal variation of the particle number size distributions (Gao et al., 2012). Over the 36-day summer campaign, there

were 13 NPF events.

Figure 6 shows two typical NPF events during the summer campaign. The events were observed on July 3 and 9, 2015, and lasted for a few hours. The temporal developments of concentration of SO_2 and particle number size distributions during the NPF events were shown in Fig. 6. In the observed NPF events, the concentration of nucleation mode particles began to increase sharply at about 10:00 h with the high concentration of SO_2, especially in July 9, 2015. When the newly formed particles grew, the concentration of nucleation mode particles began to decrease, whereas that of the Aitken mode particles continued to increase a period of time.

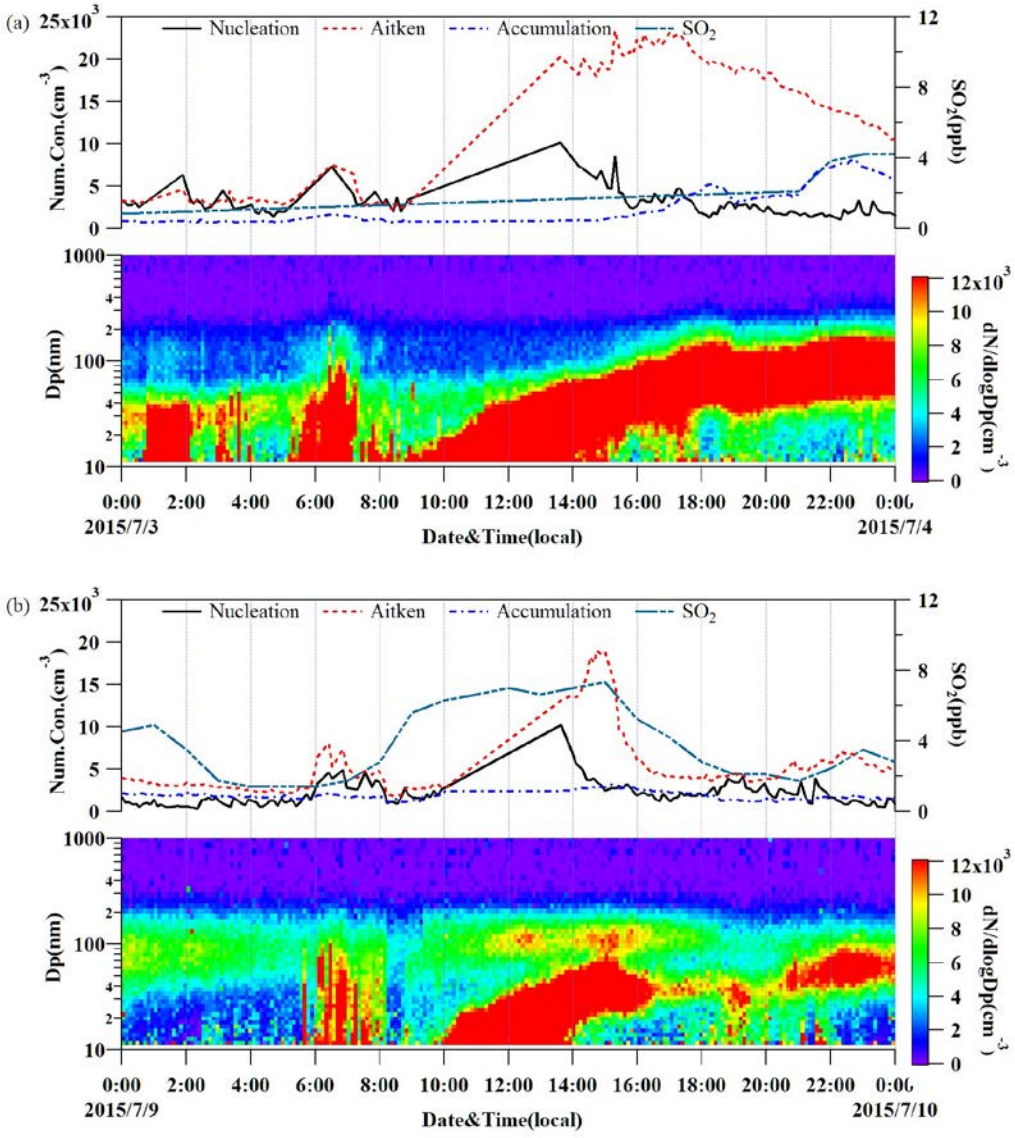

Figure 6. Time series of mass concentrations of SO_2, number concentrations nucleation mode, Aitken mode particles, accumulation mode particles and image plot of particle number size

distributions during the two typical NPF events observed on July 3 (a) and 9 (b), 2015.

The concentration of particles in nucleation and Aitken mode vary greatly during the day, but this is not the case for accumulation mode particles. The concentration of nucleation mode particles was relatively low during the nighttime (19:00 h to 6:00 h), approaching $2.0\times10^{3}cm^{-3}$, while it reached as high as $5.0\times10^{3}cm^{-3}$ during the NPF period. The lowest concentration of Aitken mode particles was observed before and during the occurrence of NPF episodes, which usually occurred under clean air conditions (Huang et al., 2017). Number concentration of Aitken mode particles was at their lowest level between 8:00 and 10:00 h, which was less than $4.0\times10^{3}cm^{-3}$. This might be induced by the development of the boundary layer, which leads to a dilution of air pollutants and a decrease in the concentration of atmospheric background particles (Liu et al., 2017). The newly formed particles grew continuously from nucleation to Aitken mode size, with a sharp decrease in the number concentration of Aitken mode particles, and the highest concentration reaching 6.0×10^{3} cm^{-3}. The accumulation mode particles were less affected by the primary emissions, and the concentration varied little in the day, remaining at about 6.0×10^{3} cm^{-3}.

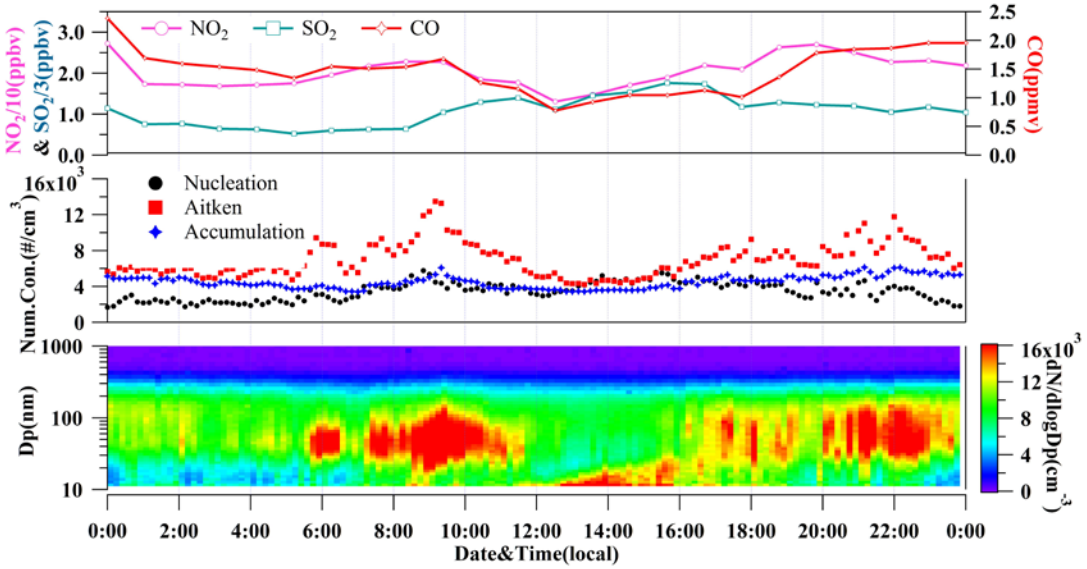

Figure 7. Average diurnal variation of NO_2, SO_2, CO concentrations and number size distributions of particles observed during the winter campaign.

Average number concentration of particles was very low from midnight to 6:00 am during the winter campaign, but that of the nucleation mode particles was similar

to that in the summer (approx. $2.0\times10^{3}cm^{-3}$). Similar to the summer morning peak, the concentration of Aitken mode particles increased rapidly at about 6:00 h in the winter and remained high until 11:30 h, when the maximum concentration was close to $1.2\times10^{4}cm^{-3}$. In the meantime, the number concentrations of accumulation and nucleation mode particles also increased significantly. The concentrations of all particles were then quickly restored to a very low level after the episode.

Five NPF events were observed but more likely to occur in the midday (from 12:00 h), with no significant increase in particle size, which may be related to the weak photochemical reaction intensity and low condensable vapor concentration in winter(Cheung et al., 2013; Wang et al., 2014a). The higher the coagulation sink (CS), the less suitable for the generation and growth of new particles (Lehtinen et al., 2003; Pirjola et al., 1999). Preexisting particles can scavenge newly formed particles and condensable vapors, thus suppress NPF. The CS in winter is generally higher than summer, as shown in Figure 8. This probably be another reason why the occurrence of NPF events in winter was much less than events in summer. During the NPF events, the particle number concentration in nucleation mode increased rapidly from $3.0\times10^{3}cm^{-3}$ to near $5.0\times10^{3}cm^{-3}$, but the period of subsequent particle growth was relatively short. It terminated at about 16:00 h when the mean size grew to about 30 nm. The variation in particle number concentration from 16:00 to 20:00 h may be related to the increase in the vehicle flow during evening rush hours(Wang et al., 2014c; Wu et al., 2008). From 20:00 h until midnight, the particle number size distributions appeared to be similar to that at 6:00 to 11:30 h. During the night, the concentration of CO was higher than that during the daytime. The northeast of the observation site is a residential area, where the residents still mainly rely on coal-fired heating, so the particle number size distributions appeared to have a longer duration of Aitken mode particles, which was likely because of local coal-fired emissions.

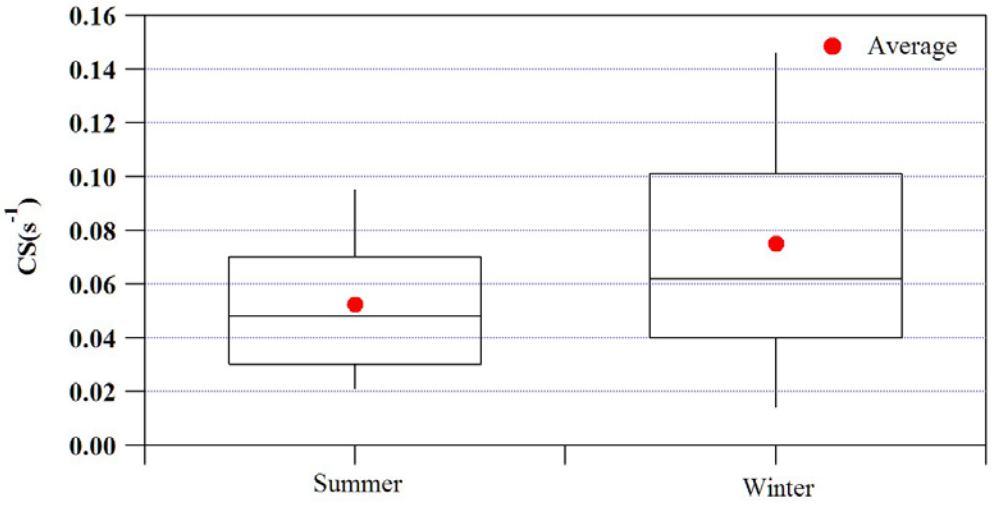

Figure 8. Box plots showing the CS during the summer and winter campaigns.

The diurnal variation in the particle number size distributions during winter was somewhat similar to that in summer. The particle number concentration in the winter ($1.5\times10^{4}cm^{-3}$) was higher than that in the summer. The Aitken mode particles were most abundant (52.2%), followed by accumulation mode (36.4%) and nucleation mode (29.6%). The main sources of Aitken mode particles are the efficient growth of nucleation mode particles and the primary emission of Aitken mode particles (Shi et al., 2007; Yue et al., 2009). However, the concentration of nucleation particles during winter was only 30% higher than that in summer, indicating that the concentration of the primary emission Aitken particles during winter is higher than that in summer, and there results were consistent with the winter coal-fired heating, biomass burning and other human activities (Liu et al., 2017).

3.3 Characteristics of particle number size distributions under different pollution conditions

To further understand the variation of particle number size distributions under different stages of hazes, pollution conditions were into three categories: 1) $PM_{2.5}<50\mu gm^{-3}$, 2) $50\leq PM_{2.5}\leq100\mu gm^{-3}$, and 3) $PM_{2.5}>l00\mu gm^{-3}$, representing three stages of the haze evolution processes – pre-haze (clean), haze formation, and haze,

respectively. Statistical variations of particle number size distributions of aerosols in the summer and the winter under different pollution conditions is shown in Figure 9. There is a shift in size distribution towards larger sizes when haze intensifies, which was also observed in Shaihai (Wang et al., 2014b). Regardless of the pollution conditions, the concentration of particles in each size segment during the winter was significantly higher than that in summer, especially for particles of <50 nm. The concentrations of particles <50 nm in the three stages duration in the winter were $6.7\times10^3 cm^{-3}$, $5.8\times10^3 cm^{-3}$ and $5.4\times10^3 cm^{-3}$, respectively, which were 46%, 54% and 98% higher than those during the summer. During the haze duration periods, concentrations of particles <50 nm in winter were almost twice those during the summer. The main reason for this phenomenon may be the winter traffic in the surrounding areas and residential coal-fired and other emissions making a high contribution to the concentrations of particles in Aitken mode (Liu et al., 2017). Particle number size distributions during the winter haze formation stage and the hazes showed a significant peak at about 50 nm, which was probably from the emissions of particles from surrounding areas (Wang et al., 2014c).

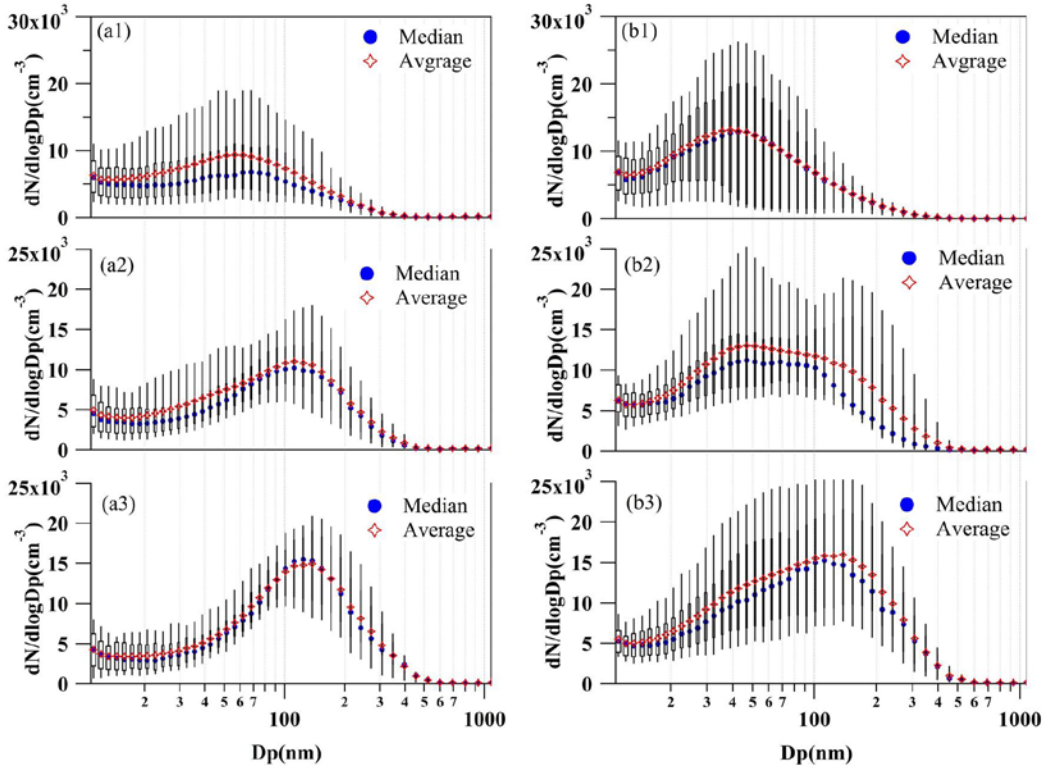

Figure 9. Box plots showing the particle number size distribution under different pollution

conditions during the summer and winter: (a1, b1) pre-haze (clean) stage, (a2, b2) haze formation stage, (a3, b3) haze stage.

.

During the pre-haze stage (before haze formation), mean particle number size distributions showed a unimodal distribution, with a peak of about 60 nm, in the summer but about 40 nm in the winter. Accumulation mode particles contributed 23% to total particle numbers in the summer, while only 15% in the winter, which was possibly due to the regional transport from the southwest pathway during the summer. Particles in the summer and winter haze formation stages showed a bimodal distribution, with peaks at ca. 50 nm and ca. 100 nm, respectively. The difference was that the primary peak is about 50 nm in the summer but 100 nm in the winter. In the winter haze formation stage, the primary peak concentration was similar to that of summer, but that of the primary peak in the winter (around 50 nm) was 48% higher than in the summer.

The distribution of particle concentration during the haze events in the summer was unimodal, with a peak between 100 and 200 nm. In contrast, it showed a bimodal distribution during the winter hazes, with one of the peaks at 100 and 200 nm, similar to that in the summer, and an additional peak at ca. 50 nm.

Table 1. Means of number concentrations of particles in different mode (in 10^3 cm^{-3}) under different pollution conditions

		Nucleation	**Aitken**	**Accumulation**	**Total Num.**
Summer	$PM_{2.5}$<50	2.3±1.5	4.8±3.8	2.1±1.4	9.2±5.5
	50≤$PM_{2.5}$≤100	1.8±1.2	4.7±2.3	3.9±1.9	10.4±4.3
	$PM_{2.5}$>100	1.4±0.8	3.9±1.2	5.5±2.3	10.8±3.2
Winter	$PM_{2.5}$<50	3.2±1.6	6.5±4.7	1.7±1.2	11.4±6.9
	50≤$PM_{2.5}$≤100	2.6±0.7	6.6±2.9	3.0±1.6	12.2±4.1
	$PM_{2.5}$>100	2.3±1.1	7.1±3.9	7.2±3.6	16.7±7.5

Table 1 showed that the difference in the total concentration of particles was not significant at different stages of typical haze events in the summer, but the proportion of each mode of particles changed substantially. The concentration of nucleation mode particles during the pre-haze stage was the highest, while it decreased significantly when the haze started to form. The varieties of particle concentration in Aitken mode were similar to those of the nucleation mode particles, while the accumulation mode particles were just the opposite. The total concentration of particles during the pre-haze stage and the haze formation stage in the winter were similar, while it increased greatly during the hazy period. Unlike in summer, the number concentration of Aitken mode particles in winter increased gradually as the haze started to form. The number concentration of nucleation mode and Aitken mode particles in the winter was generally higher than that in the same stage of summer, while the accumulation mode particles in the winter pre-haze stage and the haze formation stage was lower than those in the summer.

In summary, the size distribution towards larger sizes when haze intensifies during the both campaigns. In the three instances, particles in Aitken mode was highest for pre-haze and haze formation stage, while accumulation mode particles were predominant for haze stage.

3.4 Effects of meteorological conditions on particle number size distributions

Figure 10 shows the frequency of mean wind direction and speed from 40 to 320m in the summer and winter in Beijing. The observation site was located in the south of Yanshan Mountain, where southwest wind with a low wind speed prevails in summer, while northeast wind prevails during winter. Moreover, the air mass from the northwest is often accompanied by strong near ground wind speed, so the frequency of high wind speed during winter is relatively high.

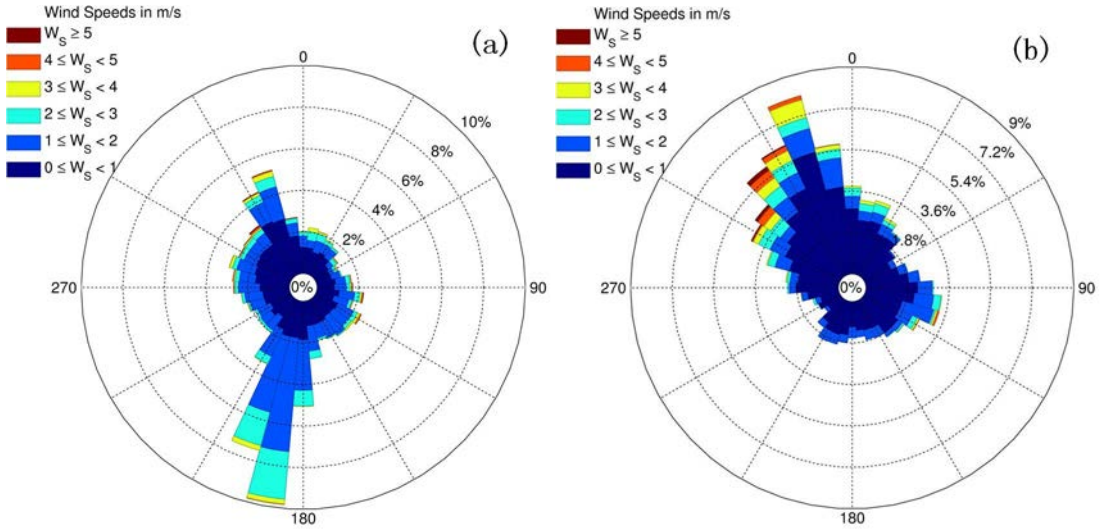

Figure 10. Mean wind direction frequency in summer (a) and winter (b) in Beijing 2015.

Figure 11 shows that concentration of particles was higher when the wind is from the south than that from the north during campaigns, especially at higher wind speeds (e.g., > 3 m/s). This is consistent with the concentration distribution characteristics of particles in the Beijing area (Liang et al., 2017; Wu et al., 2016; Zhang et al., 2017). The northern region of the observation site is mountain and forest, with limited human activities, while the southern side is in the urban area of Beijing and Hebei province. As a result, a large number of particles from Beijing and Hebei can be transported to the site under the southerly wind. In contrast, a sustained northerly wind may dilute the local particle pollution.

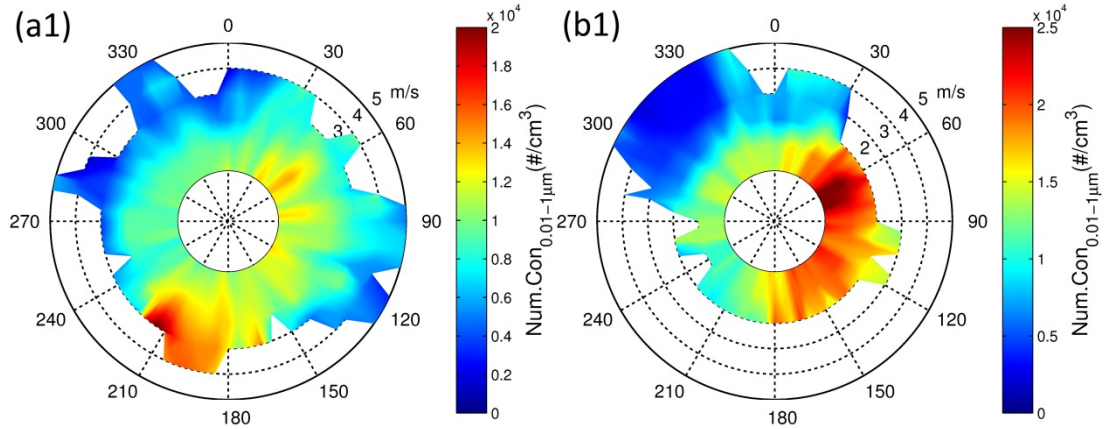

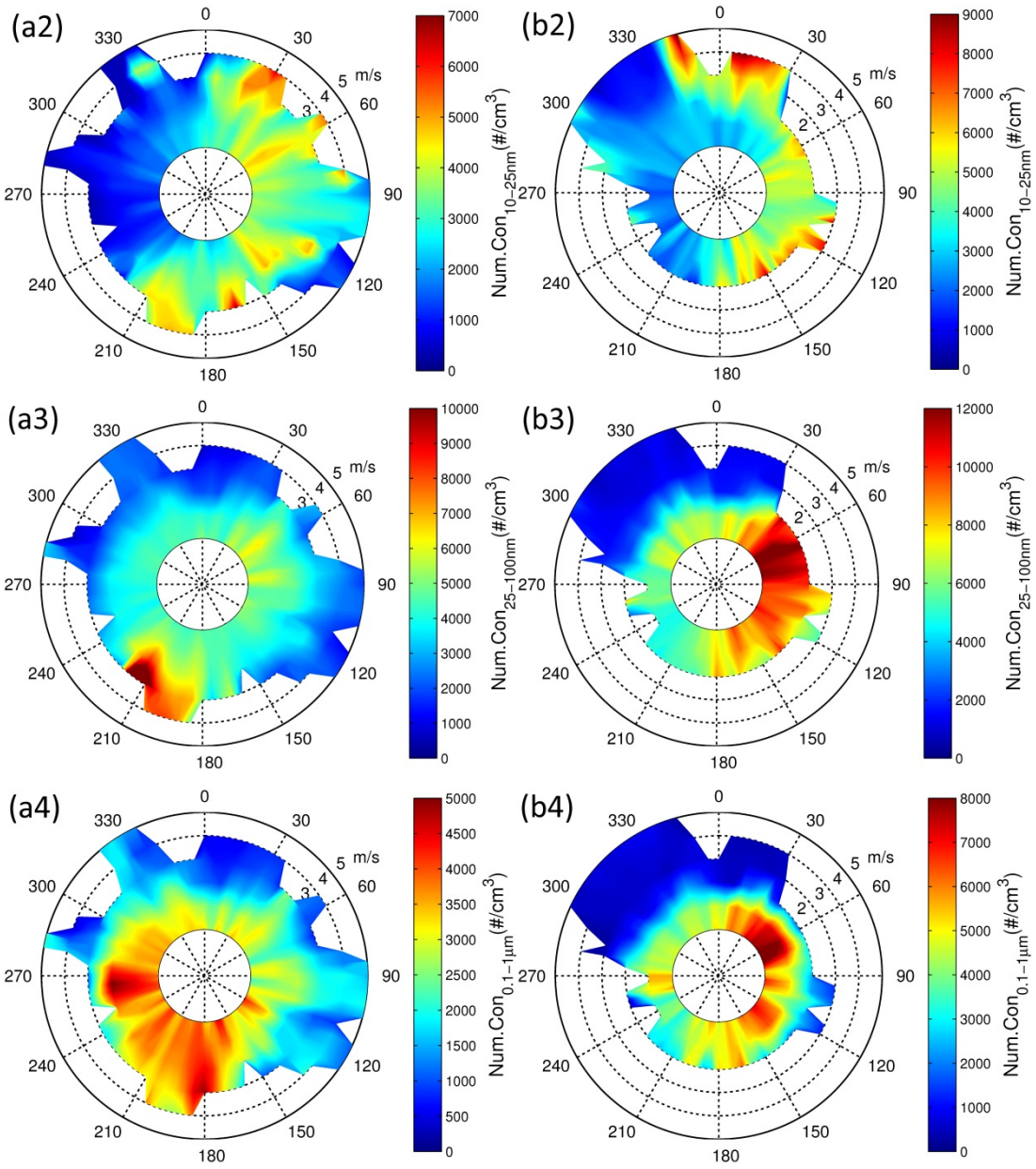

Figure 11. Polar plots for all particles (a1, b1), and particles in the nucleation (a2, b2), Aitken (a3, b3) and accumulation mode (a4, b4) during the summer and the winter, respectively.

Overall, the total concentration of particles in the summer was significantly lower than that in the winter, especially when the wind is from the northeast and southeast. However, there was no significant increase in the total concentration of particles when the wind is from the southwest. Due to the surrounding environment, the site is mainly influenced by mobile sources of vehicle emission on China National Highway 111 and stationary sources from the rural settlement across the highway. In addition, the air flow coming from the southern urban areas may bring anthropogenic emissions.

The heights of the mixing layer in the summer has a stronger effect on the dilution of particle concentration (Liu et al., 2017), which reduces the influence of traffic emissions to a certain extent. During the winter heating period, the coal-combustion activities of the nearby residential area are frequent. The concentration of CO during winter campaign was agreed with the $PM_{2.5}$ with R^2 was 0.86, and more than two times higher than that of summer, which led to a significant increase in the particle concentration of local emissions. These results suggest that the observation site is mainly affected by local emissions during the winter, but by regional transport through the southwest pathway in the summer.

The high particle concentrations in nucleation mode mainly occurred when the wind is from the north at high wind speed during both campaigns. However, when the concentration of nucleation mode particles was high, the corresponding concentrations of Aitken mode and accumulation mode were very low. These findings indicate that the northerly wind with high speed brought in clean air and plays a positive role in dilution and diffusion of the local particles, promoting NPF events.

The number concentration distribution of Aitken mode particles in the summer was significantly higher under strong southwesterly, indicating that the regional transport through the southwest passage made a large contribution to the concentration of the Aitken mode particles at the study site. The sporadic high concentration of particles under the low wind speeds when the air is from the northeast may be affected by local traffic emissions (Shi et al., 2007). The accumulation mode particles in the summer were higher when the wind is from the west and south with little difference between low and high wind speeds. This suggests that local emissions and regional transport both contributed to the concentration of particles in the accumulation mode.

The concentration of Aitken mode particles in the winter was higher primarily when the wind speed is low. It was significantly higher when the wind is from the east, which might be from the contribution from the local traffic and the coal-combustion emissions in the winter. At the same time, the concentration of accumulation mode particles was higher when the wind is from the northwest than those from the east and

southwest. Considering that the coal combustion process is more likely to produce accumulation mode particles (Liu et al., 2016; Zhang et al., 2011), it can be inferred that the residential coal-combustion in the northeast of the observation site may be a more importance source than traffic.

3.5 Air mass backward trajectory clusters

The back trajectories differed significantly between summer and winter - a majority of the air masses came from the south in the summer but from the west and northwest in the winter (Zhang et al., 2013), as shown in Figure 12.

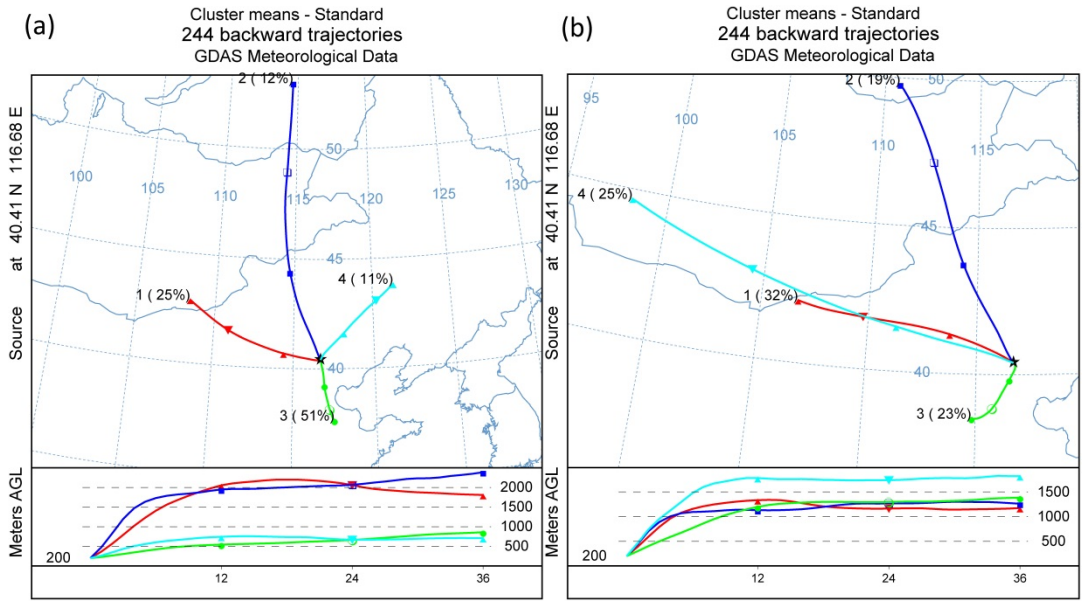

Figure 12. The 36 h back trajectories starting at 200 m above ground level in the observation site were calculated every 6 h (at 00:00, 06:00, 12:00, and 18:00 local time) during summer (a) and winter (b) in 2015.

The trajectories of air masses arriving at the observation site in the summer and winter can be divided into four categories or clusters: northwestern (NW), southwestern (including southern, SW), northern (N), and northeastern (NE) directions. Table 2 summarizes the percentage of each trajectory cluster in the winter and summer, as well as the origin and the average number concentration of each mode of particles and the total concentration corresponding to each trajectory cluster.

Table 2. The percentage and origin of each trajectory cluster and means (with one

473 standard deviation) of number concentrations of particles in each mode and total
474 number concentration ($10^3 cm^{-3}$) during summer and winter
475

		Percent (%)	Origin	Nucleation (10^3 cm^{-3})	Aitken (10^3 cm^{-3})	Accumulation (10^3 cm^{-3})	Total Num. (10^3 cm^{-3})
Summer	Cluster 1	25	NW	2.9±1.7	6.3±3.8	4.0±1.8	13.2±5.3
	Cluster 2	12	N	4.8±2.8	5.0±4.4	1.2±0.7	10.9±6.6
	Cluster 3	51	SW	2.3±1.6	4.5±1.8	3.7±2.2	10.4±4.0
	Cluster 4	11	NE	2.4±1.1	3.6±1.9	2.0±1.2	8.0±3.1
Winter	Cluster 1	32	NW	3.3±2.4	7.4±3.1	5.9±4.0	16.7±6.8
	Cluster 2	19	N	3.4±2.3	4.6±4.3	1.2±0.8	9.3±6.5
	Cluster 3	23	SW	3.2±1.3	7.7±2.6	5.1±3.1	16.1±5.2
	Cluster 4	25	NW	3.6±1.7	7.1±3.0	4.5±3.4	15.2±6.1

476

477 During the summer campaign, the trajectory of cluster 3 from SW accounted for
478 the largest proportion of all trajectories (51%), which was followed by the NW cluster
479 1 (25%), N cluster 2 (12%) and NE cluster 4 (11%). The trajectory clusters are
480 dominated by cluster 1 and cluster 4 (NW), accounting for 32% and 25% in the winter.
481 Cluster 2 (N) and cluster 3 (SW) accounted for the remainder (19 and 23%,
482 respectively).

483 Figure 13 shows that the peak size of particle number size distributions during
484 summer was 70–80 nm, 50nm, 100nm, and 60-70nm for the trajectory cluster 1, 2, 3
485 and 4, respectively. The concentration of particles was highest for trajectory cluster 1
486 and lowest for trajectory cluster 4.

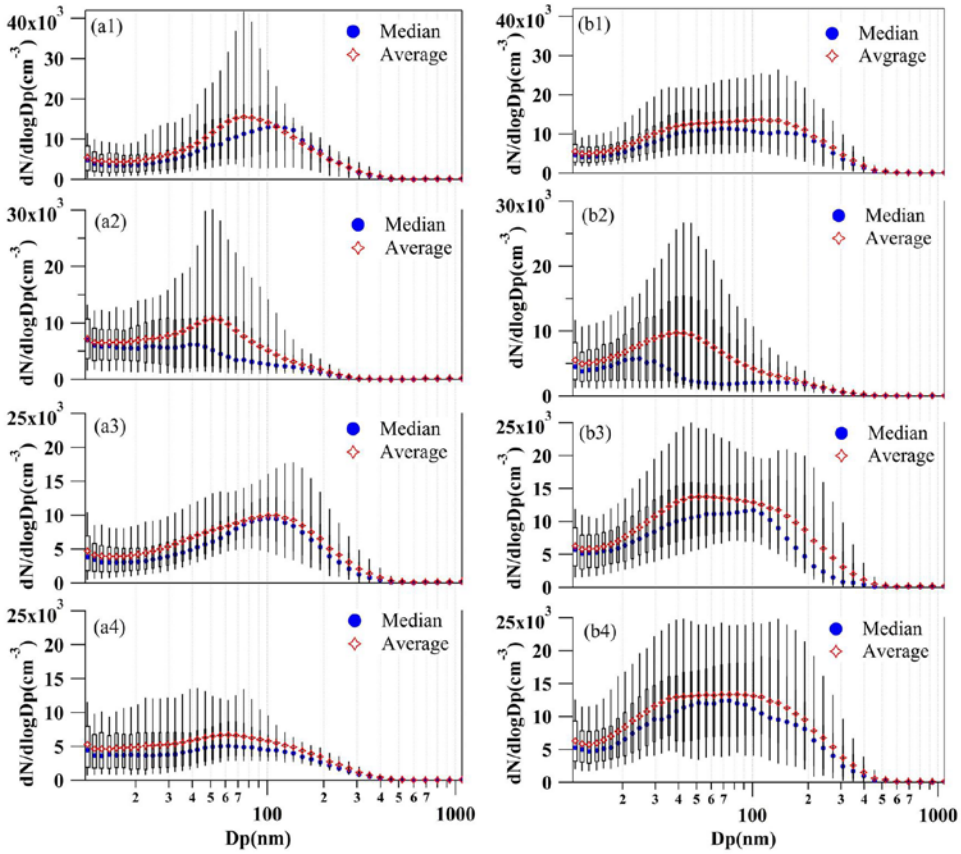

Figure 13. Box plots showing the particle number size distribution for the air back trajectory clusters during the summer and winter: (a1, b1) Cluster 1, (a2, b2) Cluster 2, (a3, b3) Cluster 3, (a4, b4) Cluster 4.

The Aitken mode and accumulation mode particles in cluster 1 during summer had the highest number concentrations (6.3×10^3 cm^{-3} and 4.0×10^3 cm^{-3}, respectively). In contrast, trajectory cluster 2 had the highest number concentration of nucleation mode particles ($4.8\times10^3 cm^{-3}$) and the lowest accumulation mode particles ($1.2\times10^3 cm^{-3}$). The trajectory cluster 1 coming from the SW direction may carry particles from the western urban areas into Beijing. The NPF event was the most important contributor to the nucleation mode particles (Wang et al., 2011; Yue et al., 2010; Zhang et al., 2011), and the concentration of the local background particles was low under the control of the cluster 2 air mass, which facilitates the occurrence of NPF events.

The peak size of particle number size distributions during winter was 110 nm, 40nm, 50-60nm, and 40-90nm for the trajectory cluster 1, 2, 3 and 4, respectively, as shown in Fig.12. The concentration of particles was highest for trajectory cluster 1

and almost the same with the trajectory cluster 3 and 4, but the lowest for trajectory cluster 2. The Aitken mode and accumulation mode particles in cluster 2 during winter had the lowest number concentrations (4.6×10^3 cm^{-3} and 1.2×10^3 cm^{-3}, respectively). It was mainly because trajectory cluster 2 originated from a clean area with short transport pathways when compared with other clusters. However, the number concentrations of nucleation mode particles in all trajectory clusters were close to each other, indicating that there may be no obvious relationship between the occurrence of NPF and the source of air mass during winter.

The concentration of particles was highest for trajectory cluster 1 during both campaigns. Trajectory cluster 2 originated from northern clean areas and had a similar particle number size distribution during both winter and summer; however, the number concentrations of nucleation mode and Aitken mode particles in summer were slightly higher than those in winter. This may have occurred because of the high frequency of NPF events during summer, as well as the more active photochemical processes, which provided high concentrations (Wang et al., 2014a; Zhao et al., 2013) of low volatility condensable vapor molecules to further promote the condensation growth of nucleation mode particles. In addition, trajectory cluster 1, 4 and 3 in winter had different origins located in northwest and southwest Beijing, and the length of the trajectories differed, although the corresponding particle number size distributions was similar. A possible explanation for this is that the particle number size distributions in winter was greatly affected by local emissions (Liu et al., 2016; Tang et al., 2015; Zheng et al., 2014).

4. Summary and conclusions

The particle number size distribution of aerosols (11.1 to 1083.3 nm) was monitored in Beijing during the HOPE-J^3A field campaign. The average number concentration of particles during the summer and winter campaigns were $9.6\pm4.8\times10^3$ cm^{-3} and $13.9\pm8.3\times10^3$ cm^{-3}, respectively. There were frequent long-duration haze events during the winter campaign. The total number concentration of particles was

44.7% higher than that in the summer, with the largest difference being in Aitken mode particles. The number concentration of particles in Aitken mode dominated during both campaigns. Particle number concentrations showed close correlations with traffic and residents living activities and wind speed, especially for the nucleation mode and Aitken mode particles. The NPF events occurred more frequently and for a longer duration in summer. There is a shift in size distribution towards larger sizes when haze intensifies during the both campaigns. The analysis of trajectory cluster combined with meteorological conditions suggest that Aitken and accumulation mode particles were mainly from regional transport during the summer campaign, but from vehicle and coal-combustion emissions during the winter campaign.

Acknowledgements

This research was supported by the Natural Science Foundation of China (91544218), the National Key Research and Development Program of China (2016YFF0103004 and 2017YFC0209504), and the Science and Technological Fund of Anhui Province for Outstanding Youth (1808085J19). ZS is funded by UK Natural Environment Research Center (NE/N007190/1). The authors acknowledge Dr. Nan Ma and Dr. WanYun Xu for helping to draw the wind rose contour.

References

An, X., Zhu, T., Wang, Z., Li, C., Wang, Y., 2007. A modeling analysis of a heavy air pollution episode occurred in Beijing. Atmospheric Chemistry & Physics 7, 3103-3114.

Anderson, T.L., Charlson, R.J., Schwartz, S.E., Knutti, R., Boucher, O., Rodhe, H., Heintzenberg, J., 2003. Atmospheric science. Climate forcing by aerosol--a hazy picture. Science 300, 1103-1104.

Andreae, M., Rosenfeld, D., 2008. Aerosol–cloud–precipitation interactions. Part 1. The nature and sources of cloud-active aerosols. Earth-Science Reviews 89, 13-41.

Bahadur, R., Praveen, P.S., Xu, Y., Ramanathan, V., 2012. Solar absorption by elemental and brown carbon determined from spectral observations. Proceedings of the National Academy of Sciences of the United States of America 109, 17366-17371.

Cao, J.J., Chow, J.C., Lee, S.C., Watson, J.G., 2013. Evolution of PM2.5 Measurements and Standards in the US and Future Perspectives for China. Aerosol & Air Quality Research 13, 1197-1211.

Chan, C.K., Yao, X., 2008. Air pollution in mega cities in China. Atmospheric environment 42, 1-42.

566 Chen, X., Wang, Z., Li, J., Chen, H., Hu, M., Yang, W., Wang, Z., Ge, B., Wang, D., 2017. Explaining
567 the spatiotemporal variation of fine particle number concentrations over Beijing and surrounding
568 areas in an air quality model with aerosol microphysics. Environmental Pollution, 1-12.
569 Cheung, H.C., Chou, C.C.K., Huang, W.R., Tsai, C.Y., 2013. Characterization of ultrafine particle
570 number concentration and new particle formation in urban environment of Taipei, Taiwan.
571 Atmospheric Chemistry & Physics 13, 8935-8946.
572 Gao, J., Chai, F., Wang, T., Wang, S., Wang, W., 2012. Particle number size distribution and new
573 particle formation: New characteristics during the special pollution control period in Beijing.
574 Journal of Environmental Sciences 24, 14-21.
575 Gao, J., Wang, T., Zhou, X., Wu, W., Wang, W., 2009. Measurement of aerosol number size
576 distributions in the Yangtze River delta in China: Formation and growth of particles under polluted
577 conditions. Atmospheric Environment 43, 829-836.
578 Han, L., Zhou, W., Li, W., 2015. Increasing impact of urban fine particles (PM2.5) on areas
579 surrounding Chinese cities. Scientific Reports 5, 1-6.
580 Heim, M., Kasper, G., Reischl, G.P., Gerhart, C., 2004. Performance of a New Commercial Electrical
581 Mobility Spectrometer. Aerosol Sci. Technol. 38, 3-14.
582 Huang, R.J., Zhang, Y., Bozzetti, C., Ho, K.F., Cao, J.J., Han, Y., Daellenbach, K.R., Slowik, J.G., Platt,
583 S.M., Canonaco, F., 2014. High secondary aerosol contribution to particulate pollution during haze
584 events in China. Nature 514, 218-222.
585 Huang, X., Wang, C., Peng, J., He, L., Cao, L., Qiao, Z., Jie, C., Wu, Z., Min, H., 2017.
586 Characterization of particle number size distribution and new particle formation in Southern China.
587 Journal of Environmental Sciences 51, 342-351.
588 Hussein, T., Puustinen, A., Aalto, P.P., Mäkelä, J.M., Hämeri, K., Kulmala, M., 2004. Urban aerosol
589 number size distributions. Atmospheric Chemistry and Physics 4, 391-411.
590 Ji, D., Li, L., Wang, Y., Zhang, J., Cheng, M., Sun, Y., Liu, Z., Wang, L., Tang, G., Hu, B., 2014. The
591 heaviest particulate air-pollution episodes occurred in northern China in January, 2013: Insights
592 gained from observation. Atmospheric Environment 92, 546-556.
593 Joshi, M., Sapra, B., Khan, A., Tripathi, S., Shamjad, P., Gupta, T., Mayya, Y., 2012. Harmonisation of
594 nanoparticle concentration measurements using GRIMM and TSI scanning mobility particle sizers.
595 Journal of Nanoparticle Research 14, 1268.
596 Kulmala, M., 2003. How Particles Nucleate and Grow. Science 302, 1000-1001.
597 Kulmala, M., Kontkanen, J., Junninen, H., Lehtipalo, K., Manninen, H.E., Nieminen, T., Petäjä, T.,
598 Sipilä, M., Schobesberger, S., Rantala, P., 2013. Direct observations of atmospheric aerosol
599 nucleation. Science 339, 943-946.
600 Kulmala, M., Riipinen, I., Sipilä, M., Manninen, H.E., Petäjä, T., Junninen, H., Maso, M.D., Mordas, G.,
601 Mirme, A., Vana, M., 2007. Toward direct measurement of atmospheric nucleation. Science 318,
602 89-92.
603 Lehtinen, K., Korhonen, H., Maso, M.D., Al, E., 2003. On the concept of condensation sink diameter.
604 Boreal Environment Research 8, 405-411.
605 Liang, P., Zhu, T., Fang, Y., Li, Y., Han, Y., Wu, Y., Hu, M., Wang, J., 2017. The Role of Meteorological
606 Conditions and Pollution Control Strategies in Reducing Air Pollution in Beijing during APEC
607 2014 and Parade 2015. Atmospheric Chemistry & Physics, 1-62.
608 Liu, Z., Hu, B., Zhang, J., Xin, J., Wu, F., Gao, W., Wang, M., Wang, Y., 2017. Characterization of fine
609 particles during the 2014 Asia-Pacific economic cooperation summit: Number concentration, size

distribution and sources. Tellus Series B-chemical & Physical Meteorology 69, 1303228.
Liu, Z., Wang, Y., Bo, H., Ji, D., Zhang, J., Wu, F., Xin, W., Wang, Y., 2016. Source appointment of fine particle number and volume concentration during severe haze pollution in Beijing in January 2013. Environmental Science & Pollution Research International 23, 6845-6860.
Mahowald, N., 2011. Aerosol indirect effect on biogeochemical cycles and climate. Science 334, 794-796.
Nel, A., 2005. Air pollution-related illness: effects of particles. Science 308, 804-806.
Parrish, D.D., Zhu, T., 2009. Clean air for megacities. Science 326, 674-675.
Pirjola, L., Kulmala, M., Wilck, M., Bischoff, A., Stratmann, F., Otto, E., 1999. Formation of Sulphuric Acid Aerosols and Cloud Condensatioan Nucleation: an Expression for Significant Nucleation and Model Comprarison. J. Aerosol Sci. 30, 1079-1094.
Quan, J., Tie, X., Zhang, Q., Liu, Q., Li, X., Gao, Y., Zhao, D., 2014. Characteristics of heavy aerosol pollution during the 2012–2013 winter in Beijing, China. Atmospheric Environment 88, 83-89.
Ramanathan, V., Crutzen, P.J., Kiehl, J.T., Rosenfeld, D., 2001. Aerosols, climate, and the hydrological cycle. Science 294, 2119.
Reischl, G.P., 1991. Measurement of Ambient Aerosols by the Differential Mobility Analyzer Method: Concepts and Realization Criteria for the Size Range Between 2 and 500 nm. Aerosol Sci. Technol. 14, 5-24.
Schäfer, K., Wang, Y., Norra, S., Shen, R., Xin, J., Ling, H., Tang, G., Münkel, C., Schleicher, N., Yu, Y., 2013. Meteorological Influences Within the Context of Air Quality in Beijing.
Shen, X., Sun, J., Zhang, Y., Wehner, B., Nowak, A., Tuch, T., Zhang, X., Wang, T., Zhou, H., Zhang, X., 2011. First long-term study of particle number size distributions and new particle formation events of regional aerosol in the North China Plain. Atmospheric Chemistry and Physics 11, 1565-1580.
Shi, Z.-b., He, K.-b., YU, X.-c., YAO, Z.-l., YANG, F.-m., Rui, M., JIA, Y.-t., ZHANG, J., 2007. Diurnal variation of number concentration and size distribution of ultrafine particles in the urban atmosphere of Beijing in winter. Journal of Environmental Sciences 19, 933-938.
Stanier, C.O., Khlystov, A.Y., Pandis, S.N., 2004. Nucleation events during the Pittsburgh Air Quality Study: description and relation to key meteorological, gas phase, and aerosol parameters special issue of aerosol science and technology on findings from the fine particulate matter supersites program. Aerosol Sci. Technol. 38, 253-264.
Sun, Y., Jiang, Q., Wang, Z., Fu, P., Li, J., Yang, T., Yin, Y., 2014. Investigation of the sources and evolution processes of severe haze pollution in Beijing in January 2013. Journal of Geophysical Research: Atmospheres 119, 4380-4398.
Sun, Y., Wang, Z., Wild, O., Xu, W., Chen, C., Fu, P., Wei, D., Zhou, L., Zhang, Q., Han, T., 2016. “APEC Blue”: Secondary Aerosol Reductions from Emission Controls in Beijing. Scientific Reports 6, 20668.
Sun, Y.L., Wang, Z.F., Du, W., Zhang, Q., Wang, Q.Q., Fu, P.Q., Pan, X.L., Li, J., Jayne, J., Worsnop, D.R., 2015. Long-term real-time measurements of aerosol particle composition in Beijing, China: seasonal variations, meteorological effects, and source analysis. Atmospheric Chemistry & Physics 15, 10149-10165.
Tang, G., Zhao, P., Wang, Y., Gao, W., Cheng, M., Xin, J., Li, X., Wang, Y., 2017. Mortality and air pollution in Beijing: The long-term relationship. Atmospheric Environment 150, 238-243.
Tang, G., Zhu, X., Hu, B., Xin, J., Wang, L., Münkel, C., Mao, G., Wang, Y., 2015. Impact of emission

controls on air quality in Beijing during APEC 2014: lidar ceilometer observations. Atmospheric Chemistry & Physics 15, 12667-12680.

Wang, D., Guo, H., Cheung, K., Gan, F., 2014a. Observation of nucleation mode particle burst and new particle formation events at an urban site in Hong Kong. Atmospheric Environment 99, 196-205.

Wang, T., Nie, W., Gao, J., Xue, L.K., Gao, X.M., Wang, X.F., Qiu, J., Poon, C.N., Meinardi, S., Blake, D., 2010. Air quality during the 2008 Beijing Olympics: Secondary pollutants and regional impact. Atmospheric Chemistry & Physics 10, 7603-7615.

Wang, X., Chen, J., Cheng, T., Zhang, R., Wang, X., 2014b. Particle number concentration, size distribution and chemical composition during haze and photochemical smoge pisodes in Shanghai. Journal of Environmental Sciences 26, 1894-1902.

Wang, Z., Hu, M., Sun, J., Wu, Z., Yue, D., Shen, X., Zhang, Y., Pei, X., Cheng, Y., Wiedensohler, A., 2013. Characteristics of regional new particle formation in urban and regional background environments in the North China Plain. Atmospheric Chemistry and Physics 13, 12495-12506.

Wang, Z.B., Hu, M., Yue, D.L., Zheng, J., Zhang, R.Y., Wiedensohler, A., Wu, Z.J., Nieminen, T., Boy, M., 2011. Evaluation on the role of sulfuric acid in the mechanisms of new particle formation for Beijing case. Atmospheric Chemistry & Physics 11, 24165-24189.

Wang, Z.B., Hu, M., Zeng, L.W., Xue, L., He, L.Y., Huang, X.F., Zhu, T., 2014c. Measurements of particle number size distributions and optical properties in urban Shanghai during 2010 World Expo: relation to air mass history. Tellus Series B-chemical & Physical Meteorology 66, 1175-1176.

Watson, J.G., 2002. Visibility: Science and regulation. Journal of the Air & Waste Management Association 52, 628-713.

Wehner, B., Wiedensohler, A., 2003. Long term measurements of submicrometer urban aerosols: statistical analysis for correlations with meteorological conditions and trace gases. Atmospheric Chemistry and Physics 3, 867-879.

Wu, Z., Hu, M., Lin, P., Liu, S., Wehner, B., Wiedensohler, A., 2008. Particle number size distribution in the urban atmosphere of Beijing, China. Atmospheric Environment 42, 7967-7980.

Wu, Z., Hu, M., Liu, S., Wehner, B., Bauer, S., ßling, A.M., Wiedensohler, A., Petäjä, T., Maso, M.D., Kulmala, M., 2007. New particle formation in Beijing, China: Statistical analysis of a 1 - year data set. Journal of Geophysical Research Atmospheres 112, D09209.

Wu, Z., Zheng, J., Shang, D., Du, Z., Wu, Y., Zeng, L., Wiedensohler, A., Hu, M., 2016. Particle hygroscopicity and its link to chemical composition in the urban atmosphere of Beijing, China, during summertime. Atmospheric Chemistry and Physics 16, 1123-1138.

Xin, J.Y., Wang, Y.S., Tang, G.Q., Wang, L.L., Yang, S., Wang, Y.H., Hu, B., Song, T., Ji, D.S., Wang, W.F., 2010. Variability and reduction of atmospheric pollutants in Beijing and its surrounding area during the Beijing 2008 Olympic Games. Chinese Science Bulletin 55, 1937-1944.

Xu, R., Tang, G., Wang, Y., Tie, X., 2016a. Analysis of a long-term measurement of air pollutants (2007–2011) in North China Plain (NCP); Impact of emission reduction during the Beijing Olympic Games. Chemosphere 159, 647-658.

Xu, X., Zhao, W., Zhang, Q., Wang, S., Fang, B., Chen, W., Venables, D.S., Wang, X., Pu, W., Wang, X., 2016b. Optical properties of atmospheric fine particles near Beijing during the HOPE-J3A campaign. Atmospheric Chemistry & Physics 16, 6421-6439.

Yue, D., Hu, M., Wu, Z., Wang, Z., Guo, S., Wehner, B., Nowak, A., Achtert, P., Wiedensohler, A., Jung, J., 2009. Characteristics of aerosol size distributions and new particle formation in the summer in Beijing. Journal of Geophysical Research Atmospheres 114, 1159-1171.

Yue, D.L., Hu, M., Zhang, R.Y., Wang, Z.B., 2010. The roles of sulfuric acid in new particle formation and growth in the mega-city of Beijing. Atmospheric Chemistry & Physics Discussions 10, 4953-4960.

Zhang, H., Hu, D., Chen, J., Ye, X., Wang, S.X., Hao, J.M., Wang, L., Zhang, R., An, Z., 2011. Particle Size Distribution and Polycyclic Aromatic Hydrocarbons Emissions from Agricultural Crop Residue Burning. Environmental Science & Technology 45, 5477-5482.

Zhang, J., Chen, Z., Lu, Y., Gui, H., Liu, J., Liu, W., Wang, J., Yu, T., Cheng, Y., Chen, Y., 2017. Characteristics of aerosol size distribution and vertical backscattering coefficient profile during 2014 APEC in Beijing. Atmospheric Environment 148, 30-41.

Zhang, R., Jing, J., Tao, J., Hsu, S.C., 2013. Chemical characterization and source apportionment of PM2.5 in Beijing: seasonal perspective. Atmospheric Chemistry & Physics 13, 7053-7074.

Zhang, X., Zhang, Y., Sun, J., Zheng, X., Li, G., Deng, Z., 2016. Characterization of particle number size distribution and new particle formation in an urban environment in Lanzhou, China. J. Aerosol Sci. 103, 53-66.

Zhao, X., Zhao, P., Xu, J., Meng, W., Pu, W., Dong, F., He, D., Shi, Q., 2013. Analysis of a winter regional haze event and its formation mechanism in the North China Plain. Atmospheric Chemistry and Physics 13, 5685-5696.

Zheng, S., Pozzer, A., Cao, C.X., Lelieveld, J., 2014. Long-term (2001-2012) fine particulate matter (PM2.5) and the impact on human health in Beijing, China. Atmospheric Chemistry & Physics Discussions 14, 5715-5725.

Zhu, X., Tang, G., Hu, B., Wang, L., Xin, J., Zhang, J., Liu, Z., Münkel, C., Wang, Y., 2016. Regional pollution and its formation mechanism over North China Plain: A case study with ceilometer observations and model simulations. Journal of Geophysical Research Atmospheres 121, 1-15.

Zhuang, X., Wang, Y., He, H., Liu, J., Wang, X., Zhu, T., Ge, M., Zhou, J., Tang, G., Ma, J., 2014. Haze insights and mitigation in China: An overview. Journal of Environmental Sciences 26, 2-12.